Jurnal Sains Kesihatan Malaysia **5** (1) 2007: 1-16

Review of X-ray Phase Contrast Imaging Techniques and Propagation Based Imaging Using a Benchtop Microfocal Source

DAVID BRADLEY, OZCAN GUNDOGDU, PAUL JENNESON, ELEFTHERIA NIRGIANAKI & ELNA HERAWATI CHE ISMAIL

ABSTRAK

Pada masa ini, asas dalam radiografi sinar-X klinikal piawai adalah penyerapan, menjejaki pengecilan sinaran apabila bim sinar-X melepasi suatu anggota badan tertentu. Proses interaksi asas adalah bergantung kepada variasi dalam nombor atom dan ketumpatan medium sasaran; akibatnya kontras radiograf boleh menjadi lemah, terutamanya untuk pengimejan tisu lembut. Beberapa tahun kebelakangan ini banyak usaha telah ditumpukan dalam penggunaan ciri fasa medan sinar-X untuk meningkatkan kontras radiografi dalam keadaan yang mencabar, terutamanya yang berkait dengan pengimejan tisu lembut. Surrey adalah salah sebuah daripada bilangan institut yang semakin bertambah dalam mana suatu program penyelidikan pengimejan sinar-X kontras fasa telah diwujudkan. Kami dengan ringkas mengkaji semula beberapa idea asas dalam pengimejan sinar-X kontras fasa dan kemudiannya menyelidiki penonjolan kontras radiografi yang dapat diperolehi, kegunaan perambatan ruang bebas yang digunakan dan menyelidiki beberapa objek kajian termasuk sampel biologi. Peralatan yang digunakan di Surrey adalah secara relatifnya mudah, mengandungi tiub sinar-X di atas bangku dengan saiz titik fokus dari beberapa mikron hingga 100 mikron dan pengesan CCD 12 bit yang sensitif kepada kedudukan.

Kata kunci: Fasa, kontras, pengimejan sinar-X.

ABSTRACT

Currently, the basis for standard clinical X-ray radiography is absorption, tracking attenuation of radiation when X-ray beams pass through a particular part of the body. The fundamental interaction processes are dependent on variations in the atomic number and density of the target medium; consequentially radiographic contrast can be poor, particularly in regard to soft tissue imaging. Over the past several years considerable interest has been paid to utilising phase properties of the X-ray field to enhance radiographic

contrast in challenging circumstances, particularly with respect to soft-tissue imaging. Surrey is among an increasing number of institutes in which a programme of investigation of phase contrast X-ray imaging has been established. We briefly review some basic ideas in X-ray phase contrast imaging and then examine the radiographic contrast enhancement that can be obtained, use being made of the method of free-space propagation and investigating a number of test objects, including biological samples. The equipment used at Surrey is relatively simple, comprising of bench-top X-ray tubes with focal spot sizes from a few microns up to 100 microns and a position sensitive 12 bit CCD detector.

Key words: Phase, contrast, X-ray imaging.

INTRODUCTION

The use of X-ray for imaging purposes has always been based on detection of contrast obtained from the difference in absorption, heavier and denser elements giving rise to a better contrast. Traditional radiology is based on a property of structural components of an object to differently absorb x-ray radiation. The contrast of a detail depends on a detail size and on a difference in absorption coefficients between the detail and environment. So, the larger is detail and/or the difference in absorption coefficients, the better is detail image on a radiograph. However, when the object mainly consists of lighter elements i.e. low Z elements or biological soft tissue, one finds that sufficient contrast can not be obtained for a good quality X-ray image as the soft tissues have close density values varying by 1 - 5%. One can employ increasing the amount of X-ray to get a better image but this would also increase the X-ray dose which is crucial in biological imaging.

During the last decade, a number of novel methods have been developed in the field of X-ray imaging which is based on the wave properties of X-rays. When X-rays pass through a weakly absorbing object, there is a phase shift occurring to X-ray beams. This allows an increase in image contrast, especially in imaging weakly absorbing samples.

There are a number of methods available for the measurement of phase shift created by the transmitted X-rays through the sample and converting them to representative images. Some of the X-ray phase contrast imaging methods require highly monochromatic plane wave radiation and sophisticated X-ray optics (Wilkins et al. 1996). However, the method adapted herein, known as propagation based phase contrast imaging but also as refraction enhanced imaging, is a relatively simple method to implement, essentially requiring only a small focus X-ray tube and electronic detection.

Phase contrast imaging techniques are being applied to a number of challenging clinical situations including mammography, bone-cartilage

radiographic imaging and lung imaging. (Lewis 2004, Majumdar et al. 2004). In the latter case, blood vessels can be clearly imaged with phase contrast imaging without the use of any contrast agents because of the difference in X-ray phase shift caused by blood and soft tissue. In addition, and in regard to tumour imaging, because of the fact that more blood vessels are created near the cancerous cells for nutrition, phase contrast might also contribute to diagnosis of cancer. Even functional imaging might be possible if a material that modulates X-ray phase tends to concentrate to a particular part or as a result of a particular condition (Momose et al. 2000).

THEORY

There are three main methods of phase imaging: the interferometric method, diffraction enhanced imaging and in-line or propagation based. These methods have either used a synchrotron or laboratory based benchtop X-ray tubes. The first two techniques requires a rather complex experimental set up compared to the latter case and it is this simplicity of the final experimental arrangement that encourages investigation of its possible implementation in clinical practice. This will be examines in details in the following sections.

When a wave interacts with matter both its amplitude and phase are modified. This change can be described by a complex form of the refractive index *n* of the medium, the value of n deviating only very slightly from unity:

$$\eta = 1 - \frac{nr_0\lambda^2}{2\pi}(f_1 + if_2) = 1 - \delta - i\beta \tag{1}$$

Here δ is the refractive index decrement due to phase shift and β describes X-ray absorption (Baruchel et al. 2000). β and the attenuation coefficient, written here as μ, are related as follows:

$$\mu = \frac{4\pi\beta}{\lambda\rho} \tag{2}$$

where λ is the wavelength and ρ is the mass density. The related phase change and attenuation on propagating a distance *x* are given by:

$$\Phi = \frac{2\pi}{\lambda}\int \delta(x)dx \quad \text{and} \quad -\log\left(\frac{I}{I_0}\right) = \frac{4\pi}{\lambda}\int \beta(x)dx \tag{3}$$

where I_0 is the incident intensity and I the final intensity. Therefore, the absorption and the phase shift of an X-ray beam propagating through an object are dependent upon both δ and β of the material being traversed (Lewis 2004).

The cross section for elastic scattering of hard X rays in matter, which causes a phase shift of the wave passing through the object of interest, is usually much greater than that for absorption. For example, 17.5-keV X rays that pass through a 50 μm thick sheet of biological tissue are attenuated by only a

fraction of a percent, while the phase shift is close to π (David et al. 2005) An important aspect of phase contrast imaging is that within the diagnostic X-ray energy range the δ of tissues is generally much greater than β (as an example, in the mammography energy range, 15-30 keV, the phase shift term δ can be 1000 times greater than the absorption term, β). Additionally, β diminishes more rapidly than δ as the incident photon energy increases, the functional dependencies being $\delta \propto E^{-2}$ and $\beta \propto E^{-4}$. As such, low dose imaging is possible since, when using absorption, soft tissue differences are only apparent at low energies (Lewis 2004).

As can be seen in Fig.1, at X-ray energies where mammography is used (15-30 keV), the phase shift term, δ, can be 1000 times greater than the absorption term, β. Therefore it might be possible to discriminate between different structures because of phase contrast where absorption is negligible (Fitzgerald 2000).

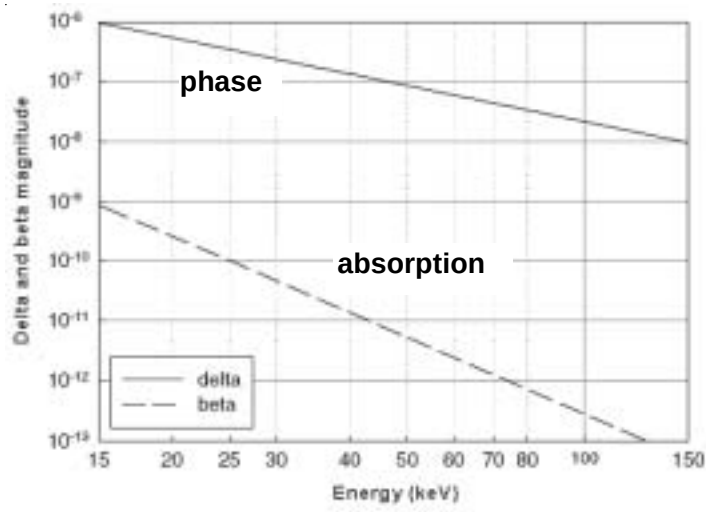

FIGURE 1. The real (δ) and imaginary (β) parts of the complex refractive index of breast tissue (Lewis 2004).

A number of different modes of X-ray phase contrast imaging has been implemented over the years, and these techniques can be classified into interferometric methods, methods using an analyser (diffraction enhanced imaging - DEI) and propagation methods, each with its advantages and disadvantages (Pfeiffer et al. 2006). They differ in the experimental setup, and the requirements on the illuminating radiation (especially its spatial coherence and monochromaticity), however the propogation method has the simplest experimental setup and does not require strict monochromacity. Fig. 2 shows the DEI imaging system schematically.

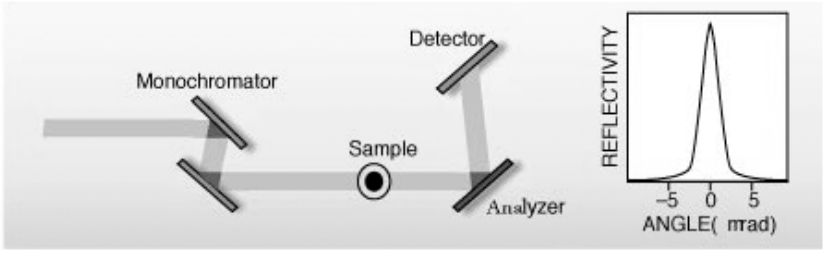

FIGURE 2. Typical set up for DEI. Variations in the refractive index of the sample generate contrast, the intensity of the X-ray beam reflected by the analyzer crystal depending on the relative angle of the incident beam with respect to the Bragg angle (Fitzgerald 2000).

The X-ray interferometric technique shown schematically in Fig.3 is complex to realise, requiring a crystal interferometer. This method is restricted to synchrotron radiation sources because of the intensity, monochromaticity and spatial coherence demanded. The incident beam is diffracted from the first silicon blade of the interferometer and splits into two coherent X-ray beams. These beams fall onto the second silicon blade that works as a mirror causing them to converge towards one another. A sample placed in the optical path of one of the beams between analyzer and mirror will create phase shifts in that beam and distort its wavefront. As a result, the recombined beams will produce interference fringes on the X-ray detector positioned behind the analyzer (Lewis 2004; Fitzgerald 2000).

For diffraction enhanced imaging (DEI) synchrotron radiation is used, the method requiring an intense beam of X-rays, with spatial and temporal coherence. DEI takes advantage of the narrow angular acceptance of Bragg reflections from perfect crystals such as silicon. A monochromatic X-ray beam from the synchrotron passes through the object and falls upon an analyzer silicon crystal. X-rays are diffracted only if they satisfy the Bragg condition, subsequently impinging onto the detector surface (see Fig. 2). The graph of diffracted X-ray intensity versus angle of the crystal is known as the 'rocking curve' and it has an approximately Gaussian shape. The diffracted X-rays from the analyzer are received by the detector and participate in the formation of an image. If the analyzer angle is set at 0° (the peak of the rocking curve) then absorption images are retrieved, free of scattered X-ray photons providing that the scatter angle is larger than the width of the rocking curve. If the angle of the analyzer is set to one yielding an intensity corresponding to half of that at the peak of the rocking curve, then the reflectivity for X-rays passing through the object undeviated is 50%. Deviated X-rays will be reflected with lower or higher efficiency depending on the angle they have when they fall upon the crystal relative to the rocking curve (Lewis 2004; Lewis et al. 2003).

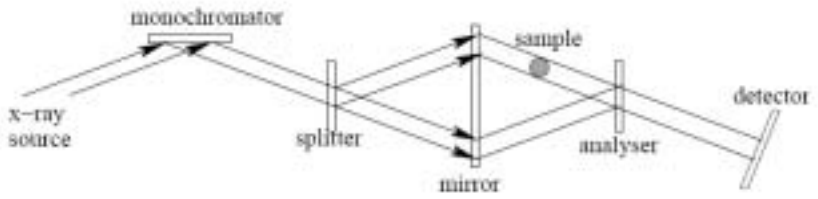

FIGURE 3. Interferometric phase imaging (Arhatari 2006).

An X-ray interferometer phase imaging is shown schematically in Fig. 3 and needs almost perfect alignment and stability of the crystals. The best results are acquired from a monolithic device in which all crystals are made from a single large ingot of crystalline silicon. Although this technique provides good stability and inherent alignment, ingot sizes limit the field of view to about 3 cm.

It has been demonstrated that DEI can produce images in which the contrast is entirely due to absorption or entirely due to changes in refractive indices in the tissue. It is also possible to construct an image containing both refraction and absorption information.

In propagation-based phase contrast (otherwise referred to as in line imaging or refraction enhanced imaging or free space propagation), a sample is put in front of the beam and the X-rays transmitted through the object at various angles will propagate over the distance between object and detector. If the detector is located directly behind the sample a conventional absorption image is obtained, while at greater distances a phase contrast image will be formed. The radiation sources that can be used must have spatial coherence (not necessarily temporal or chromatic coherence). Thus while synchrotron radiation can certainly be employed, combining spatial and temporal coherence, conventional polychromatic microfocus X-ray tubes can also be used as illustrated in Fig. 4, having sufficient spatial coherence (Snigireva et al. 2006) Phase-contrast radiography depends upon the concept of spatial coherence.

The free space propagation technique uses a unique contrast mechanism in comparison with other phase sensitive imaging techniques that has advantages concerning the simplicity of the experimental set-up. It requires no optics to form images as at X-ray wavelengths lenses are difficult to manufacture and, as there are no optical elements, produces no abberations.

In the energy range, from a few tenths to a few tens of a keV- the dominant processes include photoelectric absorption, refraction and coherent and incoherent scattering of the beam. X-ray photons travel through the object, interacting with it by photoelectric effect, Compton scattering and coherent (Rayleigh) scattering. Coherently scattered photons deflect from their initial path at small angles. This refraction of radiation occurs at the boundaries separating various media in an object of different X-ray refractive indices. At sufficiently large distances between the object and detector, the propagated

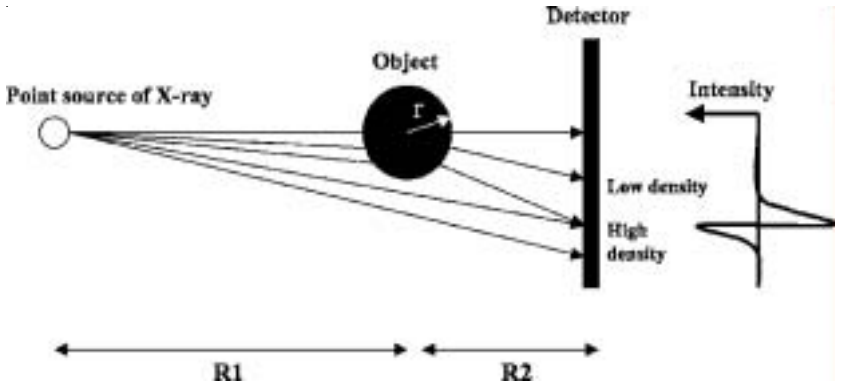

FIGURE 4. Illustration of phase contrast imaging and edge effect with a benctop X-ray point source. On the edge of the cylinder image, edge enhancement takes place due to refraction of the x-ray that is defined as phase contrast (Matsuo et al. 2004).

deflected X-ray photons can be observed to superimpose with those due to photoelectric and inelastic scatter mechanisms, producing intensity variations (Kotre & Birch 1999).

In order to achieve phase contrast imaging the X-ray tube must provide a sufficient degree of spatial or lateral coherence. A spatially-incoherent x-ray beam will not produce appreciable phase-contrast effects. Coherence, however, does not affect x-ray absorption, which is a function of the x-ray energy and object characteristics. The latter is given by:

$$d = \frac{\lambda \cdot R_1}{f} \tag{4}$$

where λ is the wavelength, R_1 is the distance between the source and the object and f is the focal spot size of the tube. Therefore phase information retrieval is easier with low energy X-ray photons, a large source to object distance and a small source size (Lewis 2004). As previously mentioned, temporal coherence or monochromaticity is not essential and as such phase contrast imaging can also be performed with polychromatic radiation (Wilkins et al. 1996).

The magnification occurring at a distance R_2 (between object and detector) is given by:

$$M = 1 + \frac{R_2}{R_1} \tag{5}$$

As a result of magnification the spatial resolution of the phase contrast images can also be improved. The image contrast obtained from the X-ray intensity profiles of an object is given by:

$$Contrast = \frac{I_{\max} - I_{\min}}{I_{\max} + I_{\min}/2} \tag{6}$$

I_{max} and I_{min} being the maximum and minimum intensities recorded across an imaged boundary. Another parameter associated with the quality of an image is the penumbra due to the finite size of the focal spot. The geometrical unsharpness is given by:

$$U_g = f\frac{R_2}{R_1} \tag{7}$$

where f is the focal spot size. It has been reported that beyond a magnification of 2x there is no further improvement in image quality; phase shifting will still be observed when edge enhancement is greater than the blurring (Kotre & Birch 1999; Matsuo et al. 2005).

In conventional radiography the primary to scatter X-ray photon ratio is improved by employing an anti-scatter grid, achieved at the cost of requiring the exposure to be increased. In phase contrast geometry an appropriate air gap R_2 is required and this can provide scatter rejection without need for a grid, possibly with lower doses being achieved. An air gap of 25 cm is considered an adequate separation for scatter elimination (Kotre & Birch 1999).

SOME KEY STUDIES

Much of the work on phase contrast imaging has bee carried out using synchrotron radiation. Momose and Fukuda (1995) utilized an X-ray interferometer to image rat cerebellar slices in the absence of a contrast agent. While in the absorption contrast image no clear structure of the cerebellum was observed, in the phase contrast image the layer structure could be seen. In addition, contrast change associated with a lipid removal procedure was investigated, a high percentage of lipid in myelin being related with improved image contrast. This suggests that phase contrast imaging may be useful in the diagnosing of demyelinating disease. In Momose et al. (2000), the ability to depict blood vessels in mouse livers without using any contrast medium was investigated, again use being made of an X-ray interferometer and synchrotron radiation. Because of the difference in X-ray phase shift caused by blood and soft tissue, trees of blood vessels were revealed in the phase contrast image.

In regard to DEI, Yagi et al. (1999) used a third generation synchrotron radiation source to allow observation of refraction of X-rays in the microradian range. The refraction produced a high contrast image of mouse lung, recorded at a distance of 6.5 m from the specimen. The images obtained were shown to be sensitive to the relative presence of air in the lung and therefore to lesions in the lung. Lewis et al. (2003) captured DEI images of mouse legs, heart, liver and

lungs. The changes of the refractive indices were greater at the boundaries of the different tissues.

In Arfelli et al. (1998) the utility of phase contrast technique in mammography was demonstrated, images of mammographic phantoms of a few centimetres thick being produced at a synchrotron for radiation doses lower or comparable to that needed in conventional mammography. Details were revealed, including thin calcium deposits and 50 μm diameter nylon wires not observed in conventional images. Phase contrast images of in vitro breast tissue specimens have subsequently been reported to provide superior image quality to conventional mammographic images (Arfelli et al. 2000).

In Matsuo et al. (2005) phase contrast images of a plastic fiber were retrieved using a micro-focus X-ray tube of 0.1 mm focal spot size. Tube voltages in the range 26 kV to 28 kV were selected, the image contrast of the plastic fiber being increased by edge enhancement. As the spatial frequency of the X-ray images increased, the sharpness gained through phase shifting also increased. Donnelly and Price (2002) evaluated polychromatic phase contrast radiography using a 0.1mm focal spot tungsten anode X-ray tube operating in the few tens of kV range. The object imaged, a sharp edge consisting of a lucite sheet of 3 mm thickness, is poorly attenuating. Phase contrast images were acquired using the free propagation technique, the image receptor being a single emulsion X-ray mammography cassette. Optical density profiles were obtained across the edge of the object using a film digitizer and X-ray refractive indices were calculated. While increase in kV caused a gradual decrease of the X-ray refractive index, the decrease was relatively small over the range of accelerating potentials studied and even at the highest potentials strong edge enhancement effects were present. Indeed, the small reduction in edge enhancement was almost certainly accompanied by a decreased radiation dose at the higher potentials.

Wu and Liu (2003) have examined design parameters and theoretical foundations in clinical implementation of X-ray phase contrast imaging. Phase contrast mammography was considered, conventional X-ray mammography being limited by sensitivity. The study indicated need for small and bright focal spot X-ray tubes, allowing sufficient spatial coherence while also providing for separations between tube and object of no greater than 1m, sufficient for manifest phase enhancement. The focal spot also needs to be sufficiently bright to allow rapid image acquisition. The design incorporated use of a film based system, offering good detector resolution for limited dynamic range. Computer simulation of the design included source to object distance, object to detector distance, magnification, X-ray tube focal spot size, kV, tube target material and filtering, entrance skin exposure, absorbed dose and acquisition time. Experiments agreed with the theoretical analysis. In particular the magnification at which maximum phase information was retrieved was 1.54x. Beyond this value the edges became blurred with loss of contrast enhancement, dose also increasing. The computer

simulations and experiments indicated it to be feasible to construct a phase contrast mammography system.

Recently Konica Minolta have developed the first digital mammography system utilising phase contrast technology (http:// konicaminolta.com /research /core_technology /mi_001.html). The magnification factor used in this REGIUS PureView mammography system is 1.75x, the system combining phase contrast mammography (PCM) and computed radiography (CR) technology, based on a molybdenum X-ray tube and a 100 µm focal spot.

PRESENT STUDIES

The experimental set up illustrated in Fig. 5, comprising an X-ray tube, a 12 bit position sensitive CCD detector and an external fan, all mounted on an optical rail enabling separations of up to 1.5 m has to be used.

FIGURE 5. Experimental set-up. From left to right is the external fan, the X-ray tube and the CCD detector.

As previously noted it is necessary for the radiation to enjoy high spatial or lateral coherence; for this reason a small focal size tube is required. The Mo anode X-ray tube used was an Oxford Instruments Series 5000 Model XTF5011 of focal spot size 110 µm, supplying anode currents from 0 to 1.0 mA and anode voltages from 4 kV to 50 kV. The cone angle of the generated beam is 25 degrees. No internal filtration and no additional external filtration was used. The detector was a Photonics Science CCD (charged couple device) model XDI camera. The light sensitive side of the semiconductor is coupled to a gadolinium oxysulphide scintillator that converts X-rays into visible light. This coupling is achieved by a direct micro-fibre optic coupling method. The XDI is a high speed, high resolution digital X-ray camera incorporating a 1330 x 1030 active pixel matrix

CCD, each pixel being 6.7 microns square. The camera offers 10 MHz or 20 MHz readout. A micro fibre-optic coupler transfers the light from an optimised scintillator input to the CCD sensor to achieve the greatest possible efficiency. Using this device, an image can be integrated for exposure times from several seconds up to several minutes for the weakest signals. The software used for retrieval of the images was Image-Pro Plus version 4.1.0.0 and the software used for the profile processing was IDL version 6.0.

RESULTS AND DISCUSSION

In line with expectation, blurring in the image increases with increase in distance between the object and detector. The geometrical unsharpness for the particular X-ray tube is shown in Fig. 6; beyond 0.7 m blurring in the image is sufficient to cause loss of edge contrast enhancement.

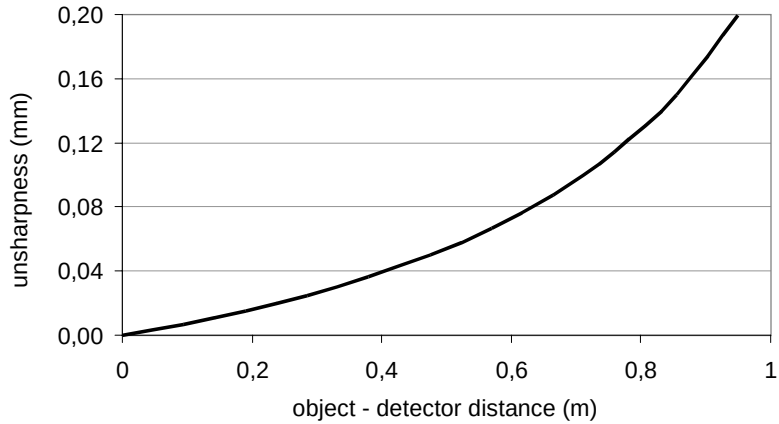

FIGURE 6. Plot of geometrical unsharpness as a function of distance between object and detector.

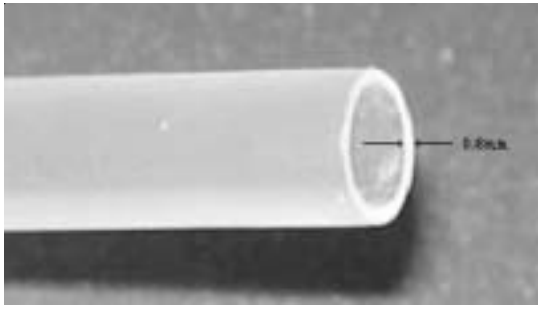

FIGURE 7. Plastic cylinder of 0.8mm wall thickness.

The first object imaged was a plastic cylinder of 0.8mm wall thickness as shown in Fig. 7. A conventional (absorption) image was first obtained, the object being located as close as possible to the window of the detector. The distance between the X-ray tube and the detector was kept at 1.5 m. Several images were subsequently retrieved, in each case altering the position of the object between the tube and the detector. Fig. 8 shows a comparison of profiles between a conventional radiograph and one obtained to provide phase contrast imaging (with a object to detector distance of 1m and source to object distance of 0.5 m. Because of the presence of quantum noise in the image, the mean of 250 profiles was calculated. This procedure was carried out using the programme IDL (Interactive Data Language).

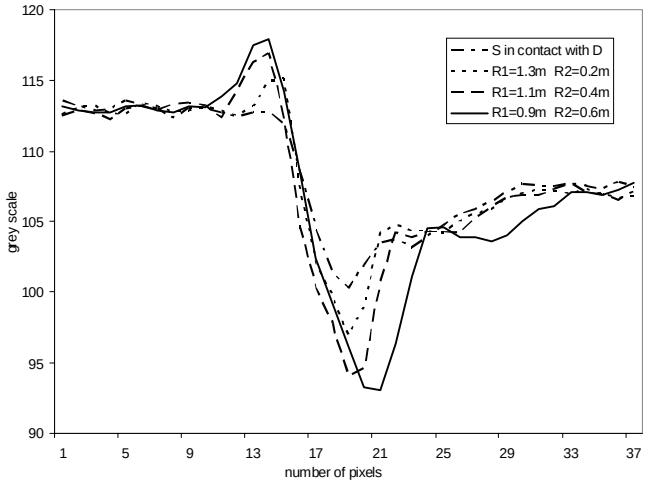

FIGURE 8. Profiles of the plastic cylinder obtained at 28 kV and 60 mAs. The alternating dash dot line is the profile of the absorption image; the solid line is the phase contrast image profile with 1.5x magnification.

To examine how contrast is modulated, the position of the object was adjusted and several profiles were calculated altering the distances R_1 and R_2 by 0.1m each time. For each image retrieved at a different position the contrast was calculated by Eqn. 6.

The contrast was calculated by Eqn 6 for each image retrieved at a different position.. The plot of the contrast versus magnification is illustrated in Fig. 9.

A drinking straw of wall thickness 0.14 mm was subsequently imaged, providing subsequently less attenuation than the original test object. The exposure conditions were 28 keV, 1 mA, exposure duration of 1min and separation between tube and detector of 1.5 m. The profiles measured in this case are shown in Fig. 10, showing significant and pronounced increase in edge contrast enhancement over the conventional image.

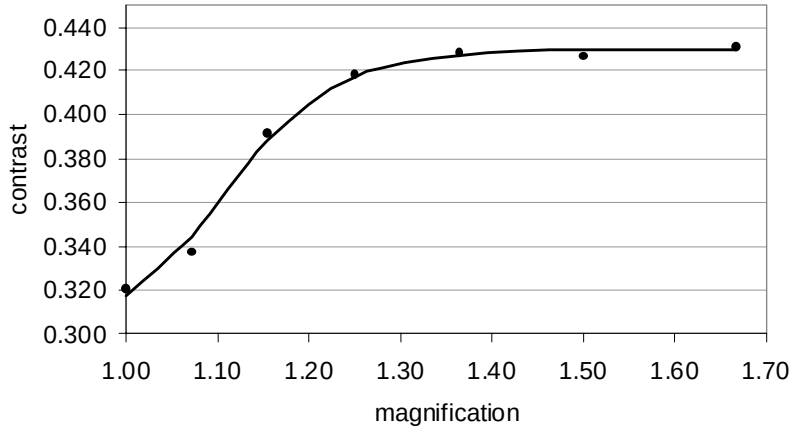

FIGURE 9. Contrast of images at different magnifications. In increasing the magnification, the contrast initially increases rapidly, subsequently achieving a plateau value for magnifications between 1.4 and 1.7x.

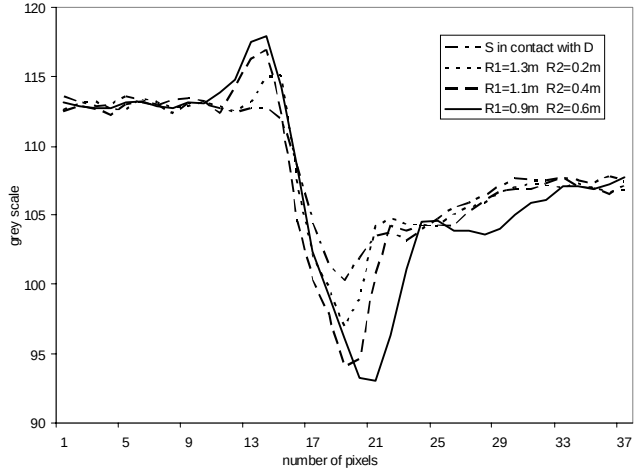

FIGURE 10. Four profiles of the plastic cylinder obtained at 28 kV and 60 mAs. The distances r_1 and r_2 were altered by 0.2m each time. As the magnification rises, the forms of the profiles change with pronounced alterations between grey scales at the edges of the object.

In addition to the above objects, a biological sample was also used to observe the results of phase contrast imaging. In particular a bee was imaged in conventional geometry (absorption image) and in phase contrast geometry (R_1 = 1 m and R_2 = 0.5 m). The difference in image quality is apparent (see Fig. 11).

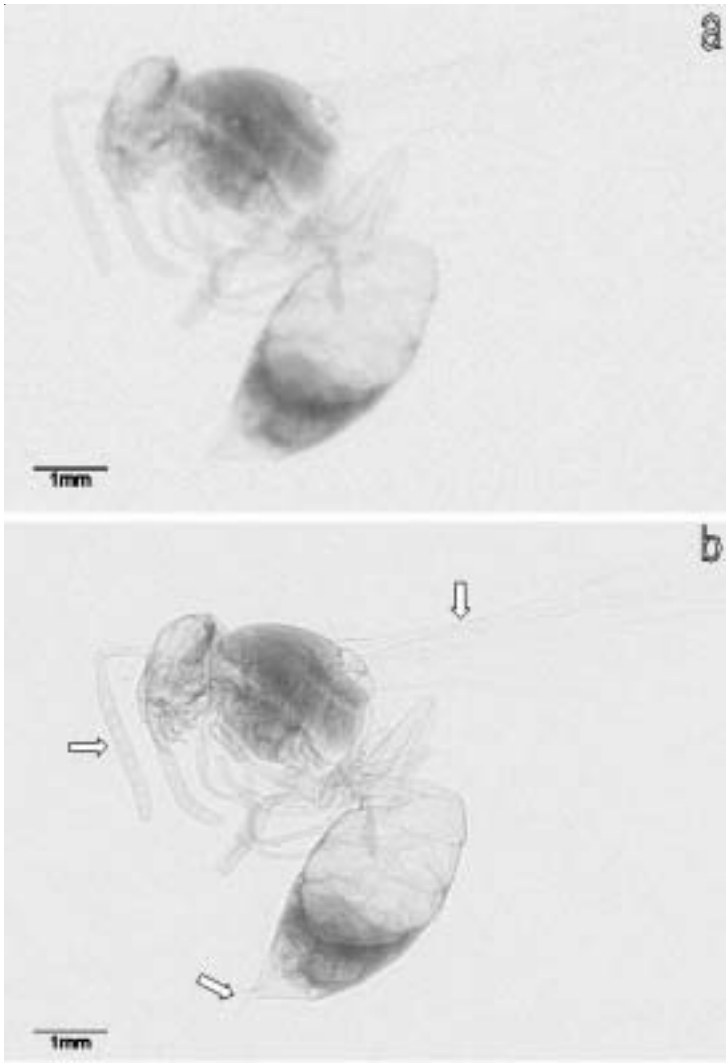

FIGURE 11. Direct comparison between the conventional absorption image (the upper image) and the phase contrast image of a bee (lower image) at 25 kV and 120 mAs with 1.5x magnification. The phase contrast image has been rescaled to its original size to allow comparison with the conventional image. Features not visible in the conventional image but apparent in the phase-enhanced image include the wings, the small chambers in the bee's antennas and the cytoskelton.

CONCLUSIONS

To-date a significant proportion of investigations of phase contrast imaging have employed synchrotron radiation, benefiting from the intensity, spatial and temporal coherence of such machines. While it is clear that there are a great range of possible applications of synchrotrons in biomedical research, the use of such facilities in patient imaging (and indeed therapeutic) studies have been rather more limited, not least because of the size, cost and availability of synchrotrons. It seems more likely that in the immediate future compact microfocus X-ray sources of high intensity will be developed as the medical imaging tool of choice. In this paper we have sought to illustrate the relative simplicity and utility of an X-ray tube-based free-space propagation method for soft-tissue imaging situations and for the study of fine detail calcified structures. We have used a 110 μm focal spot X-ray tube, characterized for contrast enhancement as a function of magnification. Subsequently we have provided examples of image enhancement.

REFERENCES

Arfelli, F., Assant, M., Bonvicini, V., Bravin, A., Cantatore, G., Castelli, E., Dalla Palma, L., Di Michiel, M., Longo, R., Olivo, A., Pani, S., Pontoni, D., Poropat, P., Prest, M., Rashevsky, A., Tromba, G., Vacchi, A., Vallazza, E. and Zanconati, F. 1998. Low-dose phase contrast X-ray medical imaging. *Phys. Med. Biol*. 43: 2845-2852.

Arfelli, F., Bonvicini, V., Bravin, A., Cantatore, G., Castelli, E., Dalla Palma, L., Di Michiel, M., Fabrizioli, M., Longo, R., Menk, R., Olivo, A., Pani, S., Pontoni, D., Poropat, P., Prest, M., Rashevsky, A., Ratti, M., Rigon, L., Tromba, G., Vacchi, A., Vallazza, E. and Zanconati, F. 2000. Mammography with Synchrotron Radiation: Phase-Detection Techniques. *Radiology* 215: 286-293.

Arhatari, B.D., "High resolution phase contrast x-ray radiography", 2006, PhD Thesis, School of Physics, University of Melbourne, Australia.

Baruchel, J., Buffiere, J., Maire, E., Merle, P. and Peix, G. 2000. X-ray tomography in material science . Hermes Science Publications: Paris.

David, C., Weitkamp, T., Khan, T., Pfeiffer, F., Bunk, O., Diaz, A., Rohbeck, T., Groso, A., Stampanoni, M. 2005. Quantitative Phase Imaging and Tomography with Polychromatic X Rays Proc. 8th Int. Conf. X-ray Microscopy, IPAP Conf. Series 7 pp. 346-348.

Donnelly, E. and Price, R. 2002. Quantification of the effect of kVp on edge-enhancement index in phase-contrast radiography. *Med. Phys*. 29: 999-1002.

Fitzgerald, R. 2000. *Phase-sensitive X-ray imaging.* Available from: http://webster-alt.aip.org/pt/vol-53/iss-7/p23.html.

Kotre, C.J. and Birch, I.P. 1999. Phase contrast enhancement of X-ray mammography: a design study. *Phys. Med. Biol*. 44: 2853-2866.

Lewis, R.A. 2004. Medical phase contrast X-ray imaging: current status and future prospects. *Phys. Med. Biol*. 49: 3573-3583.

Lewis, R.A., Hall, C.J., Hufton, A.P., Evans, S., Menk, R.H., Arfelli, F., Rigon, L., Tromba, G., Dance, D.R., Ellis, I.O., Evans, A., Jacobs, E., Pinder, S.E. and Rogers, K.D. 2003. X-ray refraction effects: application to the imaging of biological tissues. *British J. Radiol*. 76: 301-308.

Lewis, R.A., Yagi, N., Kitchen, M.J., Morgan, M.J., Paganin, D., Siu, K.K.W., Pavlov, K., Williams, I., Uesugi, K., Wallace, M.J., Hall, C. J., Whitley, J. and Hooper, S.B. 2005. Dynamic imaging of the lungs using X-ray phase contrast. *Phys. Med. Biol*. 50: 5031-5040.

Majumdar, S, Issever, A.S., Burghardt, A., Lotz, J., Arfelli, F., Rigon, L., Heitner, G., Menk, R.H., 2004. Diffraction enhanced imaging of articular cartilage and comparison with micro-computed tomography of the underlying bone structure. *European Radiology*. 14: 1440-1448.

Matsuo, S., Katafuchi, T., Tohyama, K., Morishita, J., Yamada, K. and Fujita, H. 2005. Evaluation of edge effect due to phase contrast imaging for mammography *Med. Phys*. 32: 2690-2697.

Momose, A. and Fukuda, J. 1995. Phase-contrast radiographs of nonstained rat cerebellar specimen. *Med. Phys*. 22: 375-379.

Momose, A., Takeda, T. and Itai, Y. 2000. Blood vessels: Depiction at phase-contrast X-ray imaging without contrast agents in the mouse and rat – feasibility study. *Radiology* 217: 593-596.

Pfeiffer, F., Weitkamp, T., Bunk, O. and David, C. 2006. Phase retrieval and differential phase-contrast imaging with low-brilliance X-ray sources. *Nature Physics* 2: 258-261.

Snigireva, I. and Snigirev, A. 2006. X-ray microanalytical techniques based on synchrotron radiation. *J. Environ. Monit.* 8: 33-42.

Wilkins, S.W., Gureyev, T.E., Gao, D., Pogany, A. and Stevenson, A.W. 1996. Phase contrast imaging using polychromatic hard X-rays. *Nature* 384: 335-338.

Wu, X. and Liu, H. 2003. Clinical implementation of X-ray phase contrast imaging: theoretical foundations and design considerations. *Med. Phys*. 30: 2169-2179.

Yagi, N., Suzuki, Y., Umetani, K., Kohmura, Y. and Yamasaki, K. 1999. Refraction-enhanced X-ray imaging of mouse lung using synchrotron radiation source. *Med. Phys*. 26: 2190-2193.

Bradley David
Gundogdu Ozcan
Paul Jenneson
Nirgianaki Eleftheria
Elna Herawati Che Ismail
Centre for Nuclear and Radiation Physics
Department of Physics, University of Surrey
Guildford, Surrey, GU2 7XH
United Kingdom